

06,11

On the question of the phase diagram of solid solutions

$\text{Na}_{1/2}\text{Bi}_{1/2}\text{TiO}_3-x\text{BaTiO}_3$

© L.S. Kamzina, I.P. Pronin

Ioffe Institute,
St. Petersburg, Russia

E-mail: ASKam@mail.ioffe.ru

Received May 31, 2023

Revised June 13, 2023

Accepted June 15, 2023

In solid solutions of $\text{Na}_{1/2}\text{Bi}_{1/2}\text{TiO}_3-x\text{BaTiO}_3$, the question of the relationship between the concentration of $\text{BaTiO}_3(x)$ and the presence of relaxor properties, as well as at what value of x these properties disappear, was studied. For this purpose, dielectric measurements of polarized and unpolarized compounds were carried out in a wide range of concentrations x $0.05 < x < 0.45$. Ceramic and monocrystalline samples were studied. It was found that relaxation properties exist in the studied concentration range x and the normal ferroelectric state cannot be achieved. This contradicts a number of literature data in which relaxor properties disappear already at $x = 0.18$. It is suggested that different values of x at which relaxor properties are lost may be associated with different sizes and numbers of polar nanoregions in the cubic ergodic phase resulting from the synthesis of ceramics due to different sintering temperatures and sample densities. It is concluded that the value of x , at which the relaxor properties disappear, is not constant for all NBT- x BT compounds and may vary depending on the synthesis conditions

Keywords: lead-free ferroelectrics, relaxors, phase diagram.

DOI: 10.61011/PSS.2023.09.57116.97

1. Introduction

Oxide piezoelectric materials with perovskite structure are widely used in actuators, ultrasonic motors and sensors. Regardless of the fact that piezoelectric materials based on lead zirconate titanate (PZT) have been the most preferable materials for almost five previous decades, new laws/rules led the research community to search lead-free alternatives [1]. Thus, lead-free piezoelectric materials having high electromechanical properties near the morphotropic phase boundary (MPB) were developed. One of the most promising lead-free compounds are $\text{Na}_{1/2}\text{Bi}_{1/2}\text{TiO}_3-x\text{BaTiO}_3$ (NBT- x BT) relaxors [2,3] that are transformed into ferroelectric when a strong electric field is applied. MPB between a rhombohedral and tetragonal phases in NBT- x BT exist at concentrations Ba 6–8 mol%. Despite the lower piezoelectric properties, NBT- x BT ($d_{33} \sim 150\text{--}200$ pC/N) compared with PZT and other lead-containing compounds, they have several important benefits such as easy property reproduction during synthesis and moderately high Curie temperatures. Moreover, when lead-free NBT- x BT ceramic samples are used in Langevin transducers for ultrasonic cleaning, vibration velocity was higher than that of PZT with the same input power. NBT- x BT demonstrates very stable electromechanical properties in a wide vibration velocity range. This stability is the key to the output power increase in next generation powerful devices [4,5].

Below the Burnes temperature at which polar nanoregions (PNR) occur, these nanoregions define the unusual

properties of relaxors, and more typical temperatures exist in them. The maximum permittivity temperature ($T_{\max \epsilon}$) depending on frequency, T_{FR} is the temperature of transition from ferroelectric to relaxor phase of poled samples and T_d is the depolarization temperature of pre-poled samples.

It was found in some relaxors such as 9/65/35PLZT and $\text{PbMg}_{1/3}\text{Nb}_{2/3}\text{O}_3$ (PMN) that the depolarization process has common origin with T_{FR} , and T_{FR} and T_d are identical [6,7]. At the same time, in other relaxors, including NBT and NBT-based solid solutions, T_{FR} and T_d differ from each other. It has been noted that in NBT- x BT, in particular in compounds falling on MPB, where rhombohedral and tetragonal phases coexist, T_d may be lower, higher or equal to T_{FR} depending on the content of x [8–12]. After electric field application, the induced ferroelectric state and macroscopic polarization at temperatures above T_d are damaged. The domains start vibrating due to thermal activation, but the interrelation between the local dipoles within the domains is not lost. When the sample is heated to a temperature above T_{FR} , domains are separated into polar regions and the sample changes to the relaxor state [12]. Thus, T_{FR} is the upper depolarization boundary. Such two-stage depolarization process in NBT-6BT is described in detail in [12–15]. However, other researchers [16,17] did not observe any offset between T_d and T_{FR} in NBT-6BT.

Measurements of NBT- x BT crystal samples with different x performed in [18] have shown that both scenarios are possible, because T_d and T_{FR} unnecessarily shall be identical. Different mutual arrangement of T_d and T_{FR} suggest that both direct transition to ergodic relaxor state

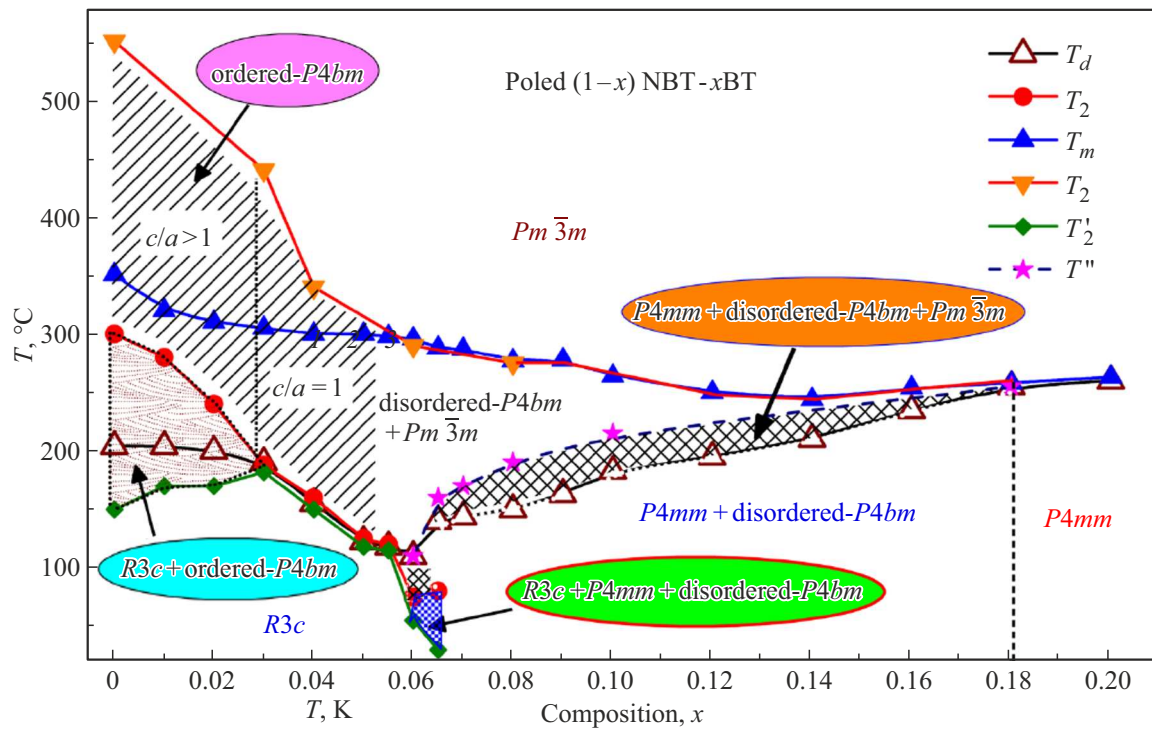


Figure 1. Phase diagram of poled $(1-x)\text{NBT}-x\text{BT}$. T_d is the depolarization temperature, T_2 is the temperature of phase transition from rhombohedral $R3c$ to tetragonal $P4bm$ phase, $T_{\max \epsilon}$ is the maximum permittivity temperature, T_1 is the temperature of transition from tetragonal $P4bm$ to cubic $Pm\bar{3}m$ phase, T_2' is the temperature corresponding to the start of the octahedral slope, T'' is the temperature of phase transition from tetragonal $P4mm$ to cubic $Pm\bar{3}m$ phase [10].

($T_d = T_{\text{FR}}$) and preliminary detexturization of domain polarization ($T_d < T_{\text{FR}}$) may cause depolarization.

In many studies [8,10,19–24], phase diagrams of dependences of typical temperature on x were built for poled and non-poled $\text{NBT}-x\text{BT}$. As an example, Figure 1 shows a phase diagram from [10] for poled samples. Similar diagram was built in the same study for nonpoled samples with the only difference that instead of T_d Vogel–Fulcher temperature (T_{VF}) is used, below which dynamic PNR are frozen. A slight difference between these diagrams, according to the study, is observed only for $x < 0.07$. At $x = 0$, T_d is lower than T_{FR} by almost 100 degrees. With increasing x , both temperatures decrease and at $x \sim 0.06$ they are virtually the same suggesting that the depolarization process is completed during ferroelectric-relaxor phase transition T_{FR} . Irregularity on the temperature dependence of permittivity at T_{FR} is attributable to the mixed contribution from the transition from rhombohedral $R3c$ phase to tetragonal $P4bm$ phase and thermal evolution of polar $P4bm$ nanoregions [11–13,21].

In addition, the phase diagram shows that compositions with $0.10 < x < 0.18$ exhibit at temperatures below T_d only tetragonal distortion with disordered polar nanoregions (PNR) of the tetragonal $P4bm$ phase and tetragonal high-temperature $P4mm$ phase regions with long-range order. Rhombohedral phase regions disappear in compositions with $x > 0.1$ already at room temperature. Above T_d ,

a relaxor phase is observed in these compositions, where disordered regions of $P4bm$ phase coexist with the cubic regions of $m\bar{3}m$ phase. When the composition approaches $x = 0.18$, the co-existence region of this relaxor phase gets narrow and the sample is transferred from the tetragonal phase directly to the cubic phase omitting the relaxor phase.

In compositions with $x > 0.06$, T_d starts growing and approaching the maximum permittivity temperature and, according to [10], at $x = 0.18$ these temperatures ($T_d = T_{\max \epsilon}$) are identical and the sample becomes a normal ferroelectric.

Principal controversy in literature is associated exactly with x at which $\text{NBT}-x\text{BT}$ solutions lose relaxor properties and become normal ferroelectrics. Thus in [19], the investigation of $\text{NBT}-x\text{BT}$ $0.1 < x < 0.9$ ceramic samples found that the ferroelectric relaxor behavior is observed in a wide concentration range of BaTiO_3 up to $x = 0.9$, whose stability decreases with increasing x . Only for compounds with very low contents of NBT ($x \sim 0.9$), normal ferroelectric- paraelectric phase transition is observed that is typical for pure BaTiO_3 . In [20], authors also have shown that T_d in $\text{NBT}-x\text{BT}$ with $x = 0.2$ does not agree with $T_{\max \epsilon}$ and relaxor behavior is observed.

Due to different and controversial conclusions as provided in [10,19,20] regarding the behavior of typical temperatures (T_{\max} , T_d and T_{FR}) in compositions with different x , and x limit at which relaxor properties disappear, an attempt is

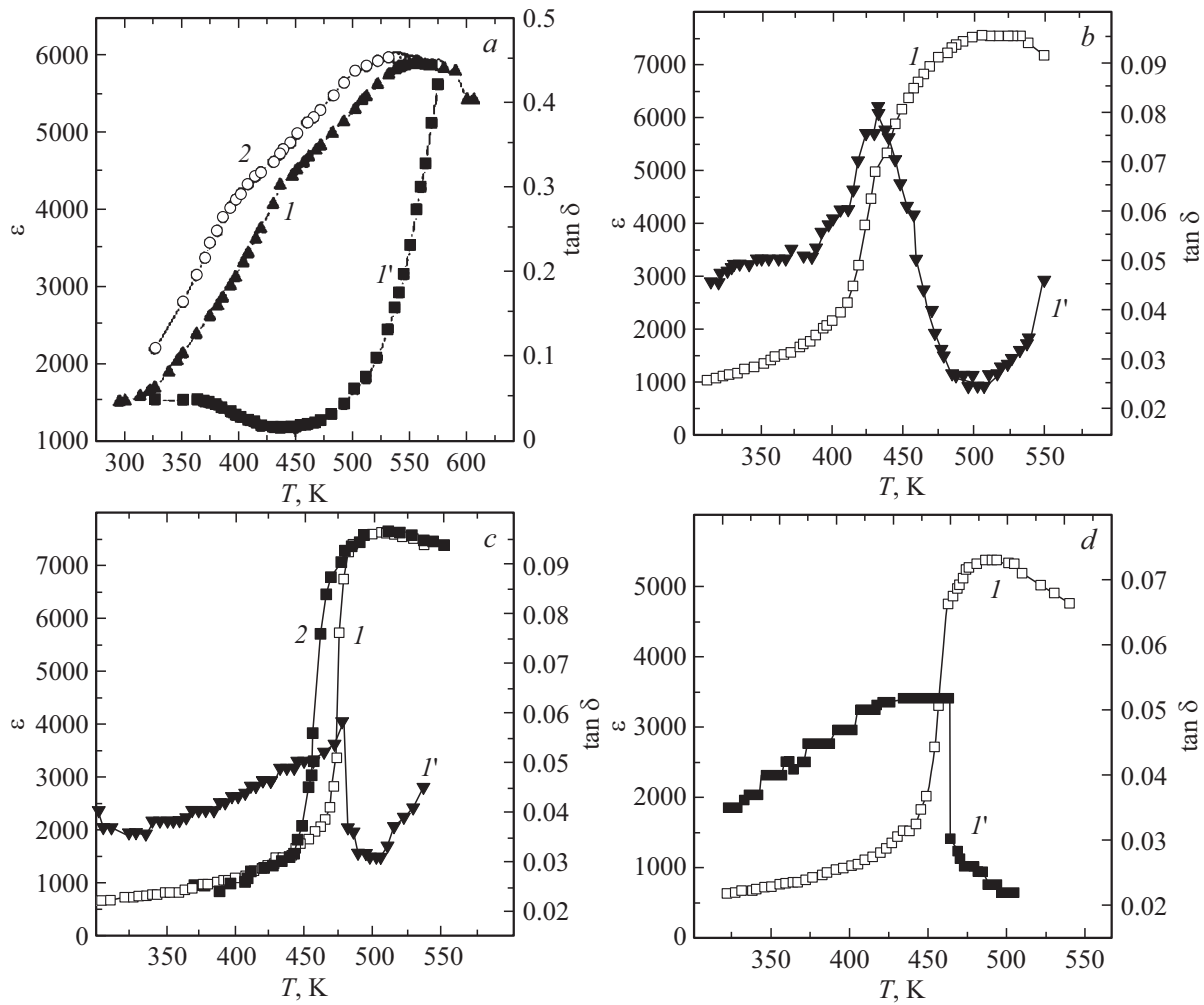


Figure 2. Temperature dependences of permittivity (ϵ) measured in heating (curves 1) and cooling (curves 2) modes and dielectric loss tangent $\tan \delta$ (curves I') for nonpoled NBT-xBT samples with different concentration Ba: $x = 0.05$ (a), $x = 0.1$ (b), $x = 0.2$ (c), $x = 0.45$ (d). Measurement frequency is 1 kHz.

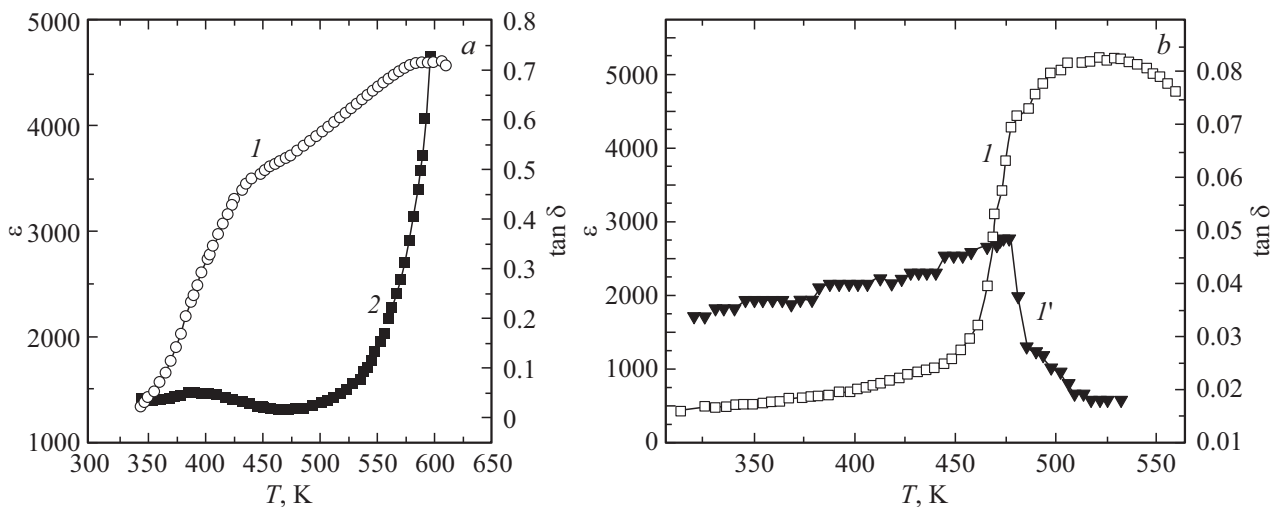


Figure 3. Temperature dependences (ϵ) (curves 1) and tangent $\tan \delta$ (curves I') measured in heating mode without electric field after application of electric field 12 kV/cm, for NBT-xBT samples with different x : $x = 0.05$ (a), $x = 0.45$ (b). Measurement frequency is 1 kHz.

made in this study to identify the presence (or absence) of relaxor properties in single-crystal and ceramic $\text{NBT}-x\text{BT}$ solid solutions in a wide concentration range of BaTiO_3 $0.05 < x < 0.45$.

2. Test samples and experimental procedure

Ceramic $\text{NBT}-x\text{BT}$ samples with Ba concentration from 10% to 45% ($0.1 < x < 0.45$) and single-crystal $\text{NBT}-0.05\text{BT}$ sample with Ba concentration 5% were studied. The ceramic samples were placed on the tetragonal side of the phase diagram, and $\text{NBT}-0.05\text{BT}$ sample was placed on the rhombohedral side. It should be reminded that MPB in $\text{NBT}-x\text{BT}$ exists at concentrations of Ba $x = 6-8$ mol%. X-ray measurements confirmed the formation of $\text{NBT}-x\text{BT}$ solid solutions in all studied compounds. In all studied samples without electric field, a macroscopic cubic phase with tetragonal symmetry regions was observed in the ceramic samples and with rhombohedral symmetry regions in $\text{NBT}-0.05\text{BT}$.

Ceramic samples with $0.1 < x < 0.45$ were prepared using a conventional ceramic process. 1–1.5 mm samples were cut from a bulk sample, polished and silver electrodes were applied on them. Growing of $\text{NBT}-0.05\text{BT}$ single-crystals is described in detail in [25]. Concentration of BaTiO_3 in initial state was determined by the atomic emission spectrometry method.

Dielectric properties of nonpoled and partially poled samples were studied. Due to technical restrictions, DC field strength applied to the sample was not higher than 15 kV/cm. Permittivity measurements were carried out at 1 kHz and 1 MHz in the temperature range 290–650 K.

3. Experimental results and discussion

Figure 2 shows the temperature dependences of permittivity (ϵ) and dielectric loss tangent ($\tan\delta$) for nonpoled samples with different concentrations of $\text{BaTiO}_3(x)$.

The Figure shows that, besides the main peak ϵ at the Curie temperature corresponding to the transition to cubic phase, a slight irregularity is observed at lower temperature in all test samples, which at low x ($x = 0.05$) occurs in the form of a small knee on curve ϵ and at high concentrations x occurs in the form of $\tan\delta$ peak. This temperature corresponds to the phase transition to the tetragonal relaxor phase (T_{FR}). It should be noted that $T_{\text{max}\epsilon}$ and T_{FR} are not identical, and the higher x , the lower the difference between them.

The irregularity at T_{FR} is more clearly pronounced in poled samples, despite the applied low fields. Figure 3, *a, b* shows temperature dependences ϵ and $\tan\delta$ in $\text{NBT}-0.05\text{BT}$ (*a*) and $\text{NBT}-0.45\text{BT}$ (*b*). In Figure 3, *a* in the sample with low concentration x , curve ϵ , besides two irregularities observed in the nonpoled sample, has a third irregularity at the depolarization temperature ($T_d \sim 395$ K),

at which the largest change of the curve slope is observed, and $\tan\delta$ has a small peak. It should be noted here that the depolarization temperature T_d is lower than T_{FR} by approximately 40 K, which agrees with the data reported for $\text{NBT}-x\text{BT}$, where $x < 0.06$ [9–13].

In Figure 3, *b* for $\text{NBT}-0.45\text{BT}$ at T_{FR} , a small knee on curve ϵ is observed and coincides with $\tan\delta$ peak. No other irregularities are observed. This coincides with the phase diagram in [8,10–12], which shows that T_d and T_{FR} coincide in compounds with $0.06 < x < 0.18$.

However, our findings as shown in Figures 2, *c, d* and 3, *b* for high concentrations x differ from the data shown on the phase diagrams for poled (Figure 1) and nonpoled samples provided in [10].

From the phase diagram (Figure 1) it follows that $\text{NBT}-x\text{BT}$ compounds with $x > 0.18$ behave as normal ferroelectrics and do not exhibit relaxor properties. Symmetry of compounds with x higher that 0.18 is purely tetragonal, and at T_{max} transition from the tetragonal phase to cubic phase occurs omitting the relaxor phase. With such composition, all typical temperatures such as T_{max} , T_d and T_{RF} , according to [10], are identical.

Our data as shown in Figures 2 and 3 do not confirm these conclusions. First, it can be clearly seen that even in compositions with sufficiently high $x = 0.45$ (Figure 3, *b*) depolarization temperature coinciding with T_{FR} (transition temperature) is below $T_{\text{max}\epsilon}$. Second, temperature hysteresis is observed for permittivity measures during heating and cooling of the sample without electric field. This data is shown in Figure 2, *c* and Figure 4. This thermal hysteresis is observed even in compositions with $x = 0.35$ (Figure 4) in a quite wide temperature range and ends at the transition temperature T_{FR} . Above this temperature, the sample with $x > 0.06$ changes from almost tetragonal phase to the relaxor phase and then at $T_{\text{max}\epsilon}$ to the cubic phase.

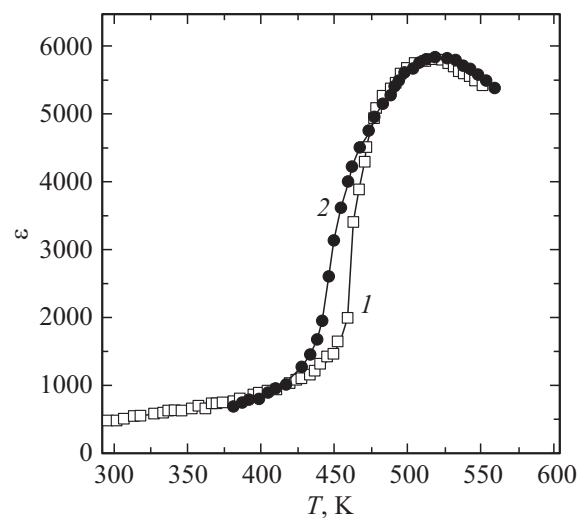


Figure 4. Temperature dependences ϵ measured in heating mode (curve 1) and cooling mode (curve 2) for $\text{NBT}-0.35\text{BT}$ sample at 1 MHz.

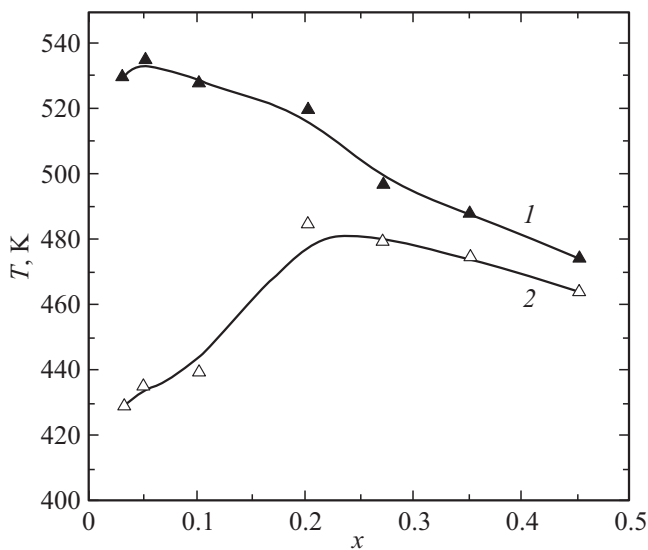


Figure 5. Concentration dependence of the maximum permittivity temperature (curve 1) and transition temperature T_{FR} (curve 2) measured at 1 kHz.

The presence of dielectric hysteresis may be explained by coexistence of tetragonal regions $P4bm$, $P4mm$ and cubic phase $m3m$ regions in this temperature range. The thermal hysteresis may suggest spontaneous 1- kind transition.

Our data agree with the conclusions in [19], where it is shown that the normal ferroelectric state occurs only in $NBT-xBT$ with $x = 0.9$, and in compositions with lower x relaxor behavior is observed.

Figure 5 shows the temperature dependence of the maximum permittivity temperature and T_{FR} on x . It can be seen that both temperatures decrease with increasing x , while $T_{\max \epsilon}$ changes faster.

The difference between $T_{\max \epsilon} - T_{FR}$ characterizing the relaxor state stability decreases with increasing $BaTiO_3(x)$. This confirms gradual transition from relaxor to normal ferroelectric state. In the ceramic samples with $x < 0.45$ studied herein, the normal ferroelectric state was not achieved.

Dielectric properties of $NBT-xBT$ with $x > 0.2$ are very similar with the properties of disordered $PbSc_{1/2}Ta_{1/2}O_3$ (PST) and $PbSc_{1/2}Nb_{1/2}O_3$ (PSN) crystals with low degree of phase transition diffusion [26,27]. In these compounds without an electric field, a spontaneous order-disorder phase transition to the ferroelectric state is observed, which is accompanied with a sharp peak on the permittivity curve. The temperature of this transition is close to the maximum permittivity temperature. In $NBT-xBT$ with $x > 0.2$, as shown in Figure 2, the phase transition at T_{FR} is followed by $\tan \delta$ peak and permittivity jump. Since the diffusion is very small, then the number and concentration of polar regions PNR in the high-temperature ergodic phase are low and PNR themselves are ordered regions. With decreasing temperature at T_{FR} , PNR may increase significantly in size up to macroscopic ferroelectric domains, and ferroelectric

interactions between PNR result in ferroelectric macroscopic order. Below T_{FR} , the ferroelectric long-range order is established.

With increasing x and x approaching 1 (pure barium titanate), the number of ordered PNR in the high-temperature phase decreases significantly and at some x , the sample from relaxor becomes a normal ferroelectric. In this case, the number of these PNR is negligible (or absent) in the cubic phase.

The question is at which x the compound is not a relaxor any more.

Controversy in x obtained herein and in [10], at which normal ferroelectric state occur and relaxor state disappears in $NBT-xBT$ solid solutions (Figure 1), may be associated with different sizes and number of polar $P4bm$ nanoregions that occur as a result of ceramic synthesis due to different sintering temperature and sample density. Therefore, x at which relaxor properties disappear is not constant for all $NBT-x$. It will change depending on the synthesis conditions.

4. Conclusions

Behavior of phase transitions in $NBT-xBT$ relaxor solid solutions was studied in a wide concentration range of $BaTiO_3(x)$ $0 < x < 0.45$, and the concentration x at which relaxor properties are lost and transition to the normal ferroelectric state takes place was investigated. It was found that the normal ferroelectric state could not be achieved in the studied concentration range x that contradicts with the findings in [10], but agrees with data in [19]. It was suggested that x at which relaxor properties are lost is not a constant value, but depends on the ceramics synthesis conditions resulting in different sizes and number of polar tetragonal nanoregions in the cubic ergodic phase.

Conflict of interest

The authors declare that they have no conflict of interest.

References

- [1] C. Herwig, H. Hofmann, G. Rowe, A. Turk. J. Eur. Union L **174**, 88 (2011).
- [2] T. Takenaka, K. Maruyama, K. Sakata. Jpn. J. Appl. Phys. **30**, 1, 2236 (1991).
- [3] V.A. Isupov. Ferroelectrics **315**, 123 (2005).
- [4] Y. Hiruma, T. Watanabe, H. Nagata, T. Takenaka. Jpn. J. Appl. Phys. **47**, 7659 (2008).
- [5] T. Tou, Y. Hamaguti, Y. Maida, H. Yamamori, K. Takahashi, Y. Terashima. Jpn. J. Appl. Phys. **48**, 07GM03 (2009).
- [6] R. Farhi, M.E. Marssi, J.L. Dellis, J-C. Picot, A. Morell. Ferroelectrics **176**, 99 (1996).
- [7] D. Viehland, M. Wuttig, L.E. Cross. Ferroelectrics **120**, 71 (1991).
- [8] F. Cordero, F. Craciun, F. Trequatrini, E. Mercadelli, C. Galassi. Phys. Rev. B **81**, 144124 (2010)

- [9] M. Slabki, L. K. Venkataraman, T. Rojac, J. Rödel, J. Koruza. *J. Appl. Phys.* **130**, 014101 (2021).
- [10] G.D. Adhikary, B. Mahale, B. N. Rao, A. Senyshyn, R. Ranjan. *Phys. Rev. B* **103**, 184106 (2021).
- [11] L.S. Kamzina. *FTT* **64**, 11, 1792 (2022) (in Russian).
- [12] E. Sapper, S. Schaab, W. Jo, T. Granzow, J. Rödel. *J. Appl. Phys.* **111**, 014105 (2012).
- [13] E.-M. Anton, W. Jo, D. Damjanovic, J. Rödel. *J. Appl. Phys.* **110**, 094108 (2011).
- [14] W. Jo, J. Daniels, D. Damjanovic, W. Kleemann, J. Rödel. *Appl. Phys. Lett.* **102**, 192903 (2013).
- [15] D. I. Woodward, R. Dittmer, W. Jo, D. Walker, D.S. Keeble, M.W. Dale, J. Rödel, P.A. Thomas, *J. Appl. Phys.* **115**, 114109 (2014).
- [16] L.M. Riemer, K.V. Lalitha, X. Jiang, N. Liu, C. Dietz, R.W. Stark, P.B. Groszewicz, G. Buntkowsky, J. Chen, S.-T. Zhang, J. Rödel, J. Koruza. *Acta Mater.* **136**, 271 (2017).
- [17] L. Kodumudi Venkataraman, T. Zhu, M. Pinto Salazar, K. Hofmann, A. Iqbal Waidha, J.C. Jaud, P.B. Groszewicz, J. Rödel. *J. Am. Ceram. Soc.* **104**, 2201 (2021).
- [18] D. Schneider, J. Rödel, D. Rytz, T. Granzow. *J. Am. Ceram. Soc.* **98**, 3966 (2015).
- [19] M. Dunce, E. Birks, M. Antonova, A. Plaude, R. Ignatans, A. Sternberg. *Ferroelectrics* **447**, 1 (2013).
- [20] Y. Hiruma, Y. Watanabe, H. Nagata, T. Takenaka. *Key Eng. Mater.* **350**, 93 (2007).
- [21] Wenwei Ge, Chengtao Luo, Qinhuai Zhang, Yang Ren, Jiefang Li, Haosu Luo, D. Viehland. *Appl. Phys. Lett.* **105**, 162913 (2014).
- [22] I. Levin, I.M. Reaney, E.M. Anton, W. Jo, J. Rödel, J. Pokorny, L. A. Schmitt, H.-J. Kleebe, M. Hinterstein, J.L. Jones. *Phys. Rev. B* **87**, 024113 (2013).
- [23] C. Ma, H. Guo, X. Tan. *Adv. Funct. Mater.* **23**, 5261 (2013).
- [24] Y. Hiruma, K. Yoshii, H. Nagata, T. Takenaka. *Ferroelectrics* **346**, 114 (2007).
- [25] Q.H. Zhang, Y.Y. Zhang, F.F. Wang, Y.J. Wang, D. Lin, X.Y. Zhao, H.S. Luo, W.W. Ge, D. Viehland. *Appl. Phys. Lett.* **95**, 102904 (2009).
- [26] F. Chu, I.M. Reaney, N. Setter. *J. Appl. Phys.* **77**, 1671 (1995).
- [27] F. Chu, N. Setter, A.K. Tagantsev. *J. Appl. Phys.* **74**, 8, 5129 (1993).

Translated by E.Ilyinskaya